A FINITE ELEMENT ANALYSIS OF CREEP DEFORMATION IN A SPECIMEN CONTAINING A MACROSCOPIC CRACK

R. Ehlers, and H. Riedel

Max-Planck-Institut für Eisenforschung, 4000 Düsseldorf,
Federal Republic of Germany

ABSTRACT

A finite element program has been developed to analyze the deformation of a creeping body that contains a stationary, macroscopic crack. The material is modelled as elastic-nonlinear viscous, i.e., the total strain rate is given by $\dot{\epsilon} = \dot{\sigma}/E + B\sigma^n$ in uniaxial tension. The program reproduces the features of the deformation field which can independently be derived by analytical methods: Near the crack tip, HRR-type stress and strain fields are obtained; in small-scale yielding (i.e., at short times after a step load is applied), a boundary layer computation yields a creep zone that grows in a self-similar manner; for long times after load application, the expected steady-state stress field characterized by the C^*-integral is attained. The transient behavior of a CT-specimen from small-scale yielding to extensive creep of the whole specimen is considered in detail. The results are compared with analytical approximations, and conclusions are drawn for fracture mechanics under creep conditions.

KEYWORDS

Finite elements, stress analysis, creep fracture, fracture mechanics.

INTRODUCTION

Failure at elevated temperature due to macroscopic creep crack growth has recently received growing attention. To develop fracture mechanics concepts for creep conditions the detailed knowledge of the stress and strain fields and their time-dependence is essential. Analytical work on this problem dealt with step-loading of a stationary crack for Mode III (Riedel, 1978) and Mode I (Riedel and Rice, 1979, and Ohji and others, 1979). The material was modelled as elastic-nonlinear viscous according to the material law $\dot{\epsilon} = \dot{\sigma}/E + B\sigma^n$ for uniaxial tension, where E is Young's modulus, and B and n are parameters of Norton's power-law creep relation. The stress and strain fields in the vicinity of the crack tip were shown to be HRR-type fields (named after Hutchinson, 1968, and Rice and Rosengren, 1968), viz.

$$\sigma_{ij} = A\, r^{-1/(n+1)}\, \tilde{\sigma}_{ij}(\theta), \qquad (1)$$

where r,θ are polar coordinates with origin at the crack tip and $\theta = o$ lying di-

rectly ahead of the crack tip; $\tilde{\sigma}_{ij}(\theta)$ is a tabulated function describing the angular dependence of the HRR-field. The load- and time-dependent stress amplitude A is given analytically for short times after load application (which ensues at the time t = o) by

$$A = \alpha_n \left[\frac{nK^2}{\pi(n+1)^2 EBt} \right]^{1/(n+1)} . \qquad (2)$$

Here, α_n is a numerical factor which is only approximately known from the analytical work. The stress intensity factor K is the relevant load parameter for short times ('small-scale yielding', abbreviated as ssy hereafter). For long times, the whole specimen creeps extensively, and a steady-state, time-independent stress field is approached. The HRR-stress amplitude is then given by

$$A = \left(\frac{C^*}{BI_n} \right)^{1/(n+1)} \qquad (3)$$

where I_n is a numerical factor given by Hutchinson (1968). The path-independent integral C^* defined by Landes and Begley (1976) is now the relevant load parameter. Riedel and Rice (1979), and Ohji and others (1979) have, somewhat arbitrarily, defined the characteristic time to distinguish between short and long times by equating the short-time and long-time stress amplitude. This leads to

$$t_1 = \frac{K^2(1-\nu^2)}{(n+1)EC^*} , \qquad (4)$$

where an approximation for the factor α_n has been made. Eq. (4) is for plane strain; for plane stress, the factor $1-\nu^2$ must be omitted.

The aim of the present study is to assess the validity of the approximation involved in the analytical short-time solution and to investigate the transient behavior of a fracture mechanics (CT-) specimen from creep on a small scale near the crack tip to extensive creep in the whole specimen. The relevance of the characteristic time for the overall specimen response is also explored. The analysis is based on the small-strain compatibility and equilibrium equations of continuum mechanics and on the elastic-nonlinear viscous material law generalized to multiaxial stress states employing Hooke's law for the elastic strain rate, and von Mises' flow rule for the creep rate, which is assumed to be incompressible.

THE FINITE ELEMENT PROGRAM

The constitutive equations have been solved by step-wise time integration following the formulation of Kanchi and others (1978). In each time step, a linear problem for the stress and strain increments, $\Delta\sigma$ and $\Delta\varepsilon$, is formulated and solved using the finite element method.

Since the instantaneous response of an elastic-nonlinear viscous body to a step-load is purely elastic, the stress field develops from an initially elastic field with the characteristic square root singularity at the crack tip. Subsequently rapid creep straining and stress relaxation take place near the tip. This behavior tends to render explicit schemes of numerical time integration unstable. Therefore the time integration is carried out in an implicit manner. The creep strain increment $\Delta\varepsilon_{ij}^{cr}$ that develops during a time increment Δt is written as a weighted sum of the inital creep rate plus the prospective creep rate at the end of the time step, times Δt. The prospective creep rate is approximated by a truncated Taylor-expansion of the creep rate around the known initial value. This leads to

$$\Delta\varepsilon_{ij}^{cr} = \Delta t[\dot{\varepsilon}_{ij}^{cr} + \chi(\partial\dot{\varepsilon}_{ij}^{cr}/\partial\sigma_{kl})\Delta\sigma_{kl}] , \qquad o < \chi \leq 1 \qquad (5)$$

where the creep rate and its derivative with respect to stress are understood at the beginning of the time step. The summation convention is applied, and χ is the weight factor. Equation (5) is a linear incremental material law relating the creep strain increment to the stress increment, $\Delta\sigma$. The elastic strain increment, $\Delta\varepsilon-\Delta\varepsilon^{cr}$, is related to $\Delta\sigma$ by Hooke's law. Further, $\Delta\sigma$ must statisfy the equilibrium equation, and the total strain increment $\Delta\varepsilon$ must be a compatible field, i.e., it is derivable from a displacement increment, Δu. Together, these requirements form a complete set of equations for the incremental quantities. From the principle of virtual displacements the finite element incremental equilibrium equation follows

$$\int_V B^T D^* B \, dV \, \Delta u = \int_V B^T D^* \dot{\varepsilon}^{cr} \Delta t \, dV - \Delta R, \qquad (6)$$

where a formulation for small strains, and the notation of Kanchi and others (1978) has been used, and ΔR is the change of external load during the increment. Since the matrix D^* depends on the partial $\partial\dot{\varepsilon}_{ij}^{cr}/\partial\sigma_{kl}$ which varies in time, the master stiffness matrix has to be recomputed in each time step. Unlike methods involving iteration this foreward gradient procedure is only conditionally stable but allows for a much larger time step than explicit methods without loss of stability or deterioration of accuracy. The initial time-increments are chosen according to the stability criterion proposed by Cormeau (1975), which yields values between $2\cdot10^{-7}$ h for plane stress and 10^{-5} h for plane strain. Empirically, it was found that, later on, the time steps can be made larger than required by the criterion by up to a factor 100 when the steady state is approached and if the 'leaping' technique suggested by Bassani and McClintock (1979) is applied. This technique means to intersperse 3 to 5 short time increments for re-stabilization after the long time steps.

Eight-noded isoparametric elements with straight edges are used throughout. At the tip, collapsed quarter-node quadrilaterals (Barsoum, 1977) are utilized. Numerical difficulties, which arise from the incompressibility of creep deformation, are dealt with by either under-integrating the element stiffness matrices (Naylor, 1974) or by using a modified variational principle (Nagtegaal and others, 1974). Both methods reproduce the (incompressible) HRR-field correctly.

In the computations, the material parameters are given the following numerical values: n=5, $B=10^{-16}$ MPa^{-5}/h, $E=1.50\cdot10^5$ MPa, Poisson's ratio $\nu=0.3$. A CT2-specimen according to ASTM E-399 is considered with crack length a=50 mm, ligament width W-a=50 mm, i.e., a/W=0.5. The applied load per specimen thickness is P=2.07 MN/m. This implies that the net section stress is $\sigma_n=P/(W-a)=41.4$ MPa, and the stress intensity factor is K=63.2 MN $m^{-3/2}$. Dimensional analysis shows that the numerical results can be applied to any other specimen size, net section stress, Young's modulus and creep coefficient B by normalizing all lengths by W, the stress field by the net section stress and the time by $1/(EB\sigma_n^{n-1})$. The stress field has the form:

$$\sigma_{ij}(r,\theta,t;\, B,E,a,W,\sigma_n,n,\nu) = \sigma_n \cdot F_{ij}\left(\frac{r}{W},\theta,\, EBt\sigma_n^{n-1};\, \frac{a}{W},n,\nu\right) . \qquad (7)$$

Here, F_{ij} is a dimensionless function of its dimensionless arguments. Note that a further reduction of the number of independent variables is possible in ssy (Riedel and Rice, 1979). In the present study no direct use is made of this latter possibility. Rather, we consider it as a check on the reliability of the finite element program if it reproduces the predicted self-similarity of the stress and strain fields in ssy.

SMALL-SCALE YIELDING

The case where large creep strains are confined to a small near-tip zone is treated as a boundary layer problem in analogy to the ssy case in elastic-plastic materials (Rice, 1968). The elastic far field is prescribed in terms of displacements on a large circle around the crack tip. The radius of the boundary layer circle has been chosen arbitrarily as r_a=5 mm, and the crack-tip element size as .0192 mm. (The finite element grid consists here of 8 equal angular sectors in the range $o<\theta<\pi$, and 14 circles centered at the crack tip, and spaced in such a manner that the element shapes are approximately quadratic except for the triangular crack-tip elements). The computation starts from the elastic stress distribution at t=o. The stress intensity factor prescribed on the boundary circle is reproduced in the near-tip region to within .5 per cent accuracy for t=o. The boundary layer computation is stopped when the stress on the boundary layer circle deviates from its linear elastic value by 10 to 15 per cent due to the development of considerable creep strain near the crack tip.

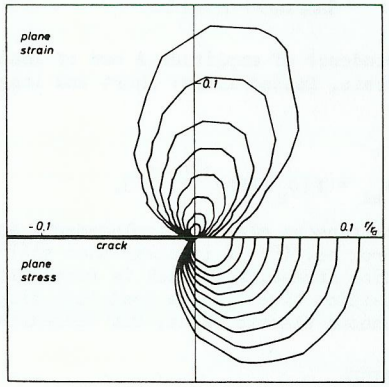

Fig. 1. Creep zone shapes in ssy in plane strain at t = .7, 2.3, 6.6, 16., 33., 61., 120., 200.$\cdot 10^{-3}$ h; in plane stress at t = 1.3, 2.2, 3.5, 5.2, 7.5, 11., 15., 21., 28.$\cdot 10^{-3}$ h.

Following Riedel (1978), and Riedel and Rice (1979), the creep zone boundary is calculated from the resulting stress and strain fields by equating the equivalent creep strain to the equivalent elastic strain. Inside the creep zone, creep strain dominates, outside elastic strain prevails. Fig. 1 shows the development of the creep zone for various time steps. After a short period of irregular initial growth not shown here, which is due to unavoidable discretization errors, a self-similar shape develops and the creep zone grows according to the time law $r_{cr} \propto t^{2/(n-1)}$ (Fig. 2). This is in accordance with the rigorous analytical conclusions of Riedel and Rice (1979). The shape of the creep zone, however, differs slightly from the shape calculated by Riedel and Rice (1979) using approximate methods. For plane strain, for example, the maximum extent of the creep zone, r_{cr}^{max}, occurs here at $\theta \approx 72^0$ compared to $\theta \approx 100^0$ according to the analytical approximation. The absolute numerical value of r_{cr}^{max} differs by some 12 per cent from the approximate analytical result (Fig. 2).

Now the numerically calculated near-tip field is compared with the analytically determined HRR-field, eq. (1), with the stress amplitude for ssy according to eq. (2). Fig. 3 shows the angular dependence of the stress component σ_{rr} for various time steps calculated on a circle around the crack tip with radius r=.0092 r_a

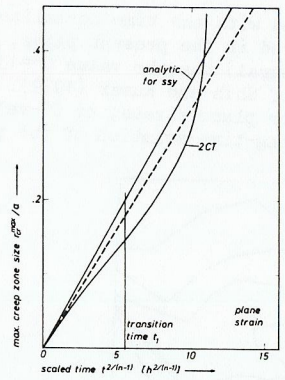

Fig. 2. Growth of creep zone in plane strain for CT-specimen. Dashed line: slope of the numerical boundary layer computation (ssy).

(second ring of elements). It is apparent that the initial elastic stress distribution develops into an HRR-type distribution, when the creep zone has grown beyond the considered ring. Also the time-dependence, $A \propto t^{-1/(n+1)}$, is reproduced well by the finite element method, and so is the radial dependence $\sigma \propto r^{-1/(n+1)}$ if the considered points lie within the creep zone. The analytical result for A, eq. (2), contains an unknown numerical factor, α_n, whose value has been estimated assuming path-independence of the J-integral (Riedel and Rice, 1979). The best fit of the numerical result for the equivalent stress to the HRR-field yields α_n=.96 for plane strain and α_n=1.05 for plane stress. This compares well with the approximate analytical results (α_n=.94 for plane strain, and α_n=1.02 for plane stress).

ANALYSIS OF THE CT-SPECIMEN

The CT-specimen is modelled using 126 isoparametric elements compared to 112 elements in the boundary layer problem described in the preceding section. The linear elastic stress intensity factor calculated with this grid at t=o deviates from the value given by Srawley (1976) by less than 1 per cent.

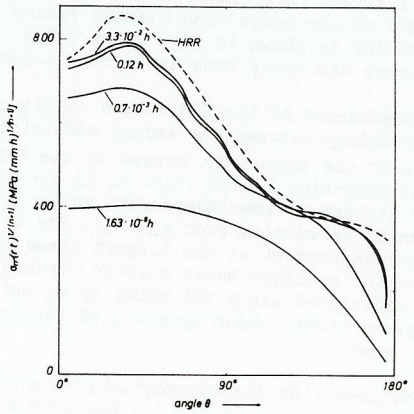

Fig. 3. Angular stress dependence in plane strain for various times. Dashed line: result of Riedel and Rice (1979).

In the following, the results are presented with the time normalized by the transition time t_1. For the CT-specimen considered in the present paper, the C^*-integral (which is entirely analogous to the J-integral) has the value $C^*=134$ N/(m·h) for plane strain according to the tabulation of Shih and Kumar (1979). Then from eq. (4) the transition time follows as $t_1=30$ h. For plane stress, no C^*-values are given in the literature for the CT-specimen. The long-time-solution of the present study yields $C^*=600$ N/(m·h) and hence $t_1=7.4$ h.

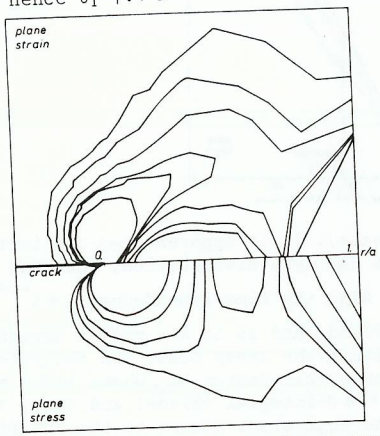

Fig. 4. Extensive creep in the CT-specimen. Creep zones in plane strain for t = 2.8, 4.1, 4.4, 5.9, 9.1, 12.8·t_1 ; in plane stress for t = 2.5, 3.8, 6.8, 9.1, 13.0·t_1.

Fig. 4 shows the development of the creep zone in the CT-specimen. For very short times ($t \lesssim 5\cdot10^{-4}$ t_1 in plane strain), the self-similar shape is observed. Of course, it is less accurately calculated here than in the boundary layer approach since the near-tip region contains less elements. For times $5\cdot10^{-4} < t/t_1 < 1$, not shown in Fig. 4, the maximum extent of the creep zone is shifted to larger angles, $\vartheta \approx 95^0$, as a consequence of the T-stress term (Larsson and Carlsson, 1974). For times greater than t_1 the growth rate of the creep zone becomes faster than predicted by the ssy calculation. This behavior is shown in Fig. 2. At $t=5.9\cdot t_1$ for plane strain and $t=13\cdot t_1$ for plane stress the creep zone has spread across the whole ligament.

In Fig. 5, the time-dependence of the HRR-stress amplitude, A, is plotted, where A is evaluated on the boundary between the second and third ring of elements (r=.46 mm) based on the best fit of the equivalent stress to the HRR-field. The analytically calculated short- and long-time limits (eqs. 2, 3) are also plotted. For long times, the stress amplitude attains a time-independent value that deviates by less than 2 per cent from the value calculated from eq. (3). The C^*-line integral turns out to be approximately path-independent at the longest times considered although there are still portions of the specimen where elastic strains cannot be neglected. The average value of C^* calculated along all paths lying entirely within the creep zone is 137 N/(m·h) for plane strain which agrees with the result of Shih and Kumar (1979), within 3 per cent.

Fig. 5 also shows the load-line displacement, Δ, as a function of the time. The particular form of the time scale, $t^{1/(n-1)}$, has been chosen so in order to draw the attention to the similarity with the Δ-vs.-load curve in elastic-plastic fracture mechanics. From the general form of the stress field, eq. (7), it follows that

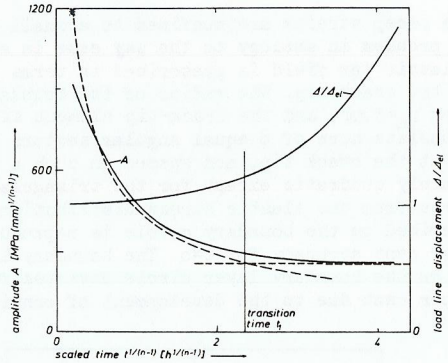

Fig. 5. Time dependence of amplitude A and of load-line displacement in plane strain. Dashed lines: short and long time limits.

$$\Delta/\Delta_{el} = f\left[\sigma_n\,(EBt)^{1/(n-1)}\right], \tag{8}$$

where Δ_{el} is the instantaneous elastic displacement, and f is an (unknown) dimensionless function. From eq. (8) it is clear that $t^{1/(n-1)}$ enters in the same way as does the net section stress, σ_n, which is proportional to the load. Fig. 5 shows that within the transition time t_1, the load-line displacement grows by 30 per cent of the instantaneous elastic value, but increases rapidly thereafter.

DISCUSSION

The similarity of the creep zone with the plastic zone in elastic-plastic materials suggests to apply the experience gathered in time-independent fracture mechanics to fracture mechanics under creep conditions. In particular, we consider the ASTM-criterion for ssy, $a > 2.5(K/\sigma_y)^2$, here. In order to make the creep zone size equal to the plastic zone size it is necessary to identify the yield stress, σ_y, with $1.6[(n+1)EBt]^{-1/(n-1)}$ in ssy. Substituting this expression for σ_y in the ASTM-criterion shows that the ASTM-limit is reached after 1.8 h for the CT-specimen considered here. Alternately, the analogy to elastic-plastic behavior can be based on equal stresses near the crack tip. This requires that the hardening exponent, N, is identified with 1/n, and σ_y with $[(n+1)EBt]^{-1/(n-1)}$. With this substitution for σ_y the ASTM-limit is reached after .28 h. According to Fig. 5, the ssy approximation for the near-tip stress amplitude in plane strain is accurate to 5, 6, and 14 per cent at the respective times t=.28 h, 1.8 h, and t_1=30 h. Considering the uncertainties involved in any fracture mechanics testing under creep conditions, each of these errors appears to be tolerable. Therefore it is suggested to apply the small-scale yielding approximation up to the time t_1, and to use the long-time solution for times $t>t_1$. A more accurate representation of the numerical results (better than 5 per cent) can be obtained by combining the short- and long-time solutions (eqs. 2, 3) as

$$A = \left[\frac{C^*(1+t_1/t)}{BI_n}\right]^{1/(n+1)} \quad \text{for} \quad 0 < t < \infty. \tag{9}$$

CONCLUSIONS

A finite element study of the time-dependent stress and strain fields at a macroscopic, stationary crack in an elastic-nonlinear viscous material has been carried out. The numerical results are confirmed by previous analytical studies. The conclusions are:

(1) The shape of the creep zone in ssy is slightly different from the shape calculated previously using approximate analytical methods. The conjecture of Riedel and Rice (1979) that the J-integral be approximately path-independent in ssy is confirmed within the accuracy of the numerical calculation.

(2) There is a close, although not rigorous, analogy between the development of the creep zone and the plastic zone in elastic-plastic fracture mechanics if the yield stress is identified with the quantity $(EBt)^{-1/(n-1)}$ times a numerical factor.

(3) Dimensional considerations suggest to plot the load-line displacement in a particular way versus time. The Δ/Δ_{el}-vs.-$\sigma_n t^{1/(n-1)}$-curve resembles the Δ/Δ_{el}-vs.-load-curve in elastic-plastic fracture mechanics.

(4) The practical meaning of the transition time t_1, somewhat arbitrarily defined in previous papers, is corroborated. After the transition time, the effect of the growing creep zone is felt at the load pins in terms of load-line displacement to an extent exceeding 30 per cent of the instantaneous elastic displacement.

(5) The near-tip stress fields can be represented to a good degree of accuracy in the whole time-range by modifying the C^*-integral in the long time solution as $C^* \cdot (1+t_1/t)$, eq. (9).

Acknowledgement. R. Ehlers was supported in this work by the Deutsche Forschungsgemeinschaft under contract Ri 329/7.

REFERENCES

Barsoum, R.S. (1977). Int. J. Num. Methods Eng. 11, 85-98.
Bassani, J.L., and McClintock, F.A. (1979). Micromechanical Modeling of Microstructural Damage in Creeping Alloys. MIT Progress Report, Dept. of Energy Contract EG-77-S-02-4461.A001, 15-20.
Cormeau, I. (1975). Int. J. Num. Methods Eng., 9, 109-127.
Hutchinson, J.W. (1968). J. Mech. Phys. Solids, 16, 13-31.
Kanchi, M.B., Zienciewicz, O.C., and Owen, D.R.J. (1978). Int. J. Num. Methods Eng., 12, 169-181.
Landes, J.D., and Begley, J.A. (1976). ASTM STP 590, American Society for Testing and Materials, Philadelphia, 128-148.
Larsson, S.G., and Carlsson, A.J. (1973). J. Mech. Phys. Solids, 21, 263-277.
Nagtegaal, J.C., Parks, D.M., and Rice, J.R. (1974). Computer Methods in Appl. Mech. Eng., 4, 153-177.
Naylor, D.J. (1974). Int. J. Num. Methods Eng., 8, 443-460.
Ohji, K., Ogura, K., and Kubo, S. (1979). Stress-strain field and modified J-integral in the vicinity of a crack tip under transient creep conditions. Paper presented at the 57th JSME National Meeting.
Rice, J.R. (1968). J. Appl. Mech., 35, 379-386.
Rice, J.R., and Rosengren, G.F. (1968). J. Mech. Phys. Solids, 16, 1-12.
Riedel, H. (1978). Z. Metallkunde, 69, 755-760.
Riedel, H., and Rice, J.R. (1979). Brown University Report E(11-1)3084/64.
Shih, C.F., and Kumar, V. (1979), Estimation Technique for the Prediction of Elastic Plastic Fracture of Structural Components of Nuclear Systems. First Semiannual Report for EPRI, Contract RP 1237-1.
Srawley, J.F. (1976). Int. J. Fracture, 12, 475-476.